Charge transfer and percolation in alkali-metal alloys

R. Avci and C. P. Flynn

Physics Department and Materials Research Laboratory, University of Illinois, Urbana, Illinois 61801

(Received 18 January 1979)

We report a comprehensive investigation of charge transfer from host to solute atoms in alloys based on alkali metals. The residual resistances of strongly electronegative impurities in quench-condensed dilute alloys clearly indicate the formation of the charge-transfer state. The same effects cause percolative transitions to random insulating phases in more concentrated alloys. In these materials, named *charge-transfer insulators*, charge transfer depletes the conduction-electron density below the level needed for charge percolation. Bounded domains of the insulating phase are observed in CsSn, NaSn, and CsAu disordered solids. Values of the minimum metallic conductivity close to the theoretical prediction $(3 \times 10^4 \ \Omega/\square)^{-1}$ are identified by the temperature dependence of conductivity close to the transitions.

I. INTRODUCTION

Impurities in alkali metals display a fascinating variety of unusual properties. In this and other respects the alkali host lattices recommend themselves highly for fundamental studies of impurity structure. They are, for example, nearly free-electron-like metals with cohesive properties that have been uniquely well understood for many years. Unfortunately, the alkali metals offer little solid- or liquid-state solubility for most impurities at ordinary temperatures. As a result, both experiment and theory in this area have been neglected, and the novel properties of the alkali alloys largely overlooked.

The problem of preparing these alloys has now been solved. Almost any desired disordered solid alloy can be fabricated by coevaporation of the components onto a substrate maintained near liquid-helium temperatures. In this paper, and in the one that follows (referred to herein as II), we report further results of a program in which the properties of these interesting systems are being investigated.

For the main part, the new properties exhibited by alkali alloys can be predicted from the characteristics of the atoms. The alkalies are large atoms, and the metals therefore have low conduction-electron densities and small Fermi energies. Impurities can introduce energy balances in which local properties overwhelm the translational energy that determines impurity structure in most commonly studied alloys (based, for example, on noble metals or aluminum). In this limit, the local potential function causes configurational effects to play a major role. We shall show that strongly electronegative impurities often occur as negative ions in alkali-metal host lattices. These effects have striking consequences for the transport prop-

erties. In particular, the charge transfer from host to impurity can induce transitions to new conduction-electron deficient insulating phases. These phases will be called charge-transfer insulators in what follows.

Up to the present time, the main evidence defining the range of conditions under which ionic configurations may be expected has been theoretical rather than experimental. It was assumed in early work on liquid-alkali-metal–alkali-halide mixtures that the halogen did, in fact, exist in solution as a negative ion.[1] Anomalies were discovered in impurity-induced spin-flip scattering by Asik, Ball, and Slichter[2] and in giant impurity diamagnetism by Flynn and Rigert,[3] both in dilute liquid alloys. These results caused the latter authors to suggest that charge transfer may have important consequences for halogen, chalcogen, and even pnictide impurities, although experimental data for these cases were mainly lacking. Theoretical calculations by Flynn and Lipari[4] using Hermann-Skillman and RPA methods, confirm that the $5p^6$ orbitals of Xe^0, I^-, and Te^{2-} impurities fall well below the conduction band of the host, namely, potassium, and that Sb^{3-} $5p^6$ orbitals fall near the band edge. An absence of conduction-band mixing with core levels is needed for true ionic behavior to occur, and this situation evidently prevails in a variety of alkali alloys. It was later shown in calculations by Flynn[5] that the *total* energies lie lowest for the ionic configurations, thereby indicating that these do indeed form the ground state of the metal-impurity complex.

No comprehensive investigation of alkali alloys has appeared since that time, either in the area of impurity properties or of more concentrated alkali alloys. Rare-gas impurities have been studied in a number of solid alkali hosts at low temperature.[6,7] The percolative transitions they induce to

the insulating state at high concentrations have been carefully documented.[7] Some results for impurity resistance in the case of low valence solutes in liquid alkalis are also known,[8] but for these cases the results have not been explained in a quantative way. Transport measurements have revealed major anomalies in the behavior of CsSb (Ref. 9) and CsAu (Ref. 10) liquid alloys near the compositions of intermetallic compounds in the solid, and an ionic component of conduction has been detected.[11] However, a systematic survey capable of revealing the scope of these effects has been lacking.

The purpose of the present work is to establish the general characteristics of alkali alloys containing various second components. Impurity properties in dilute alloys, and the behavior of concentrated alloys, are of equal interest here. Since the metallic properties are of particular concern, methods were devised to prepare solid alloys at low temperatures where thermally activated electronic and lattice conduction are both suppressed. It turned out that a simple elaboration of the methods developed in earlier studies of rare-gas impurities was adequate for this purpose.[6] These methods are discussed briefly in Sec. II of the present paper. Results of resistance measurements on a wide variety of alkali alloys are presented in Sec. III. The chosen second components include one whole row of the Periodic Table in Cs (Ag, Cd, In, Sn, Sb, Te, I, Xe, and Cs), so that the dependence of scattering power on impurity species is clearly revealed. Investigations of concentrated systems, also described in Sec. III, reveal that transitions to insulating phases occur when charge transfer reduces the number of conduction electrons below the value required for percolation. All the results are discussed in Sec. IV.

A second aspect of the same problem is deferred to Paper II of the present series. This is the question of excited-state structure. A spectroscopy of locally excited impurity valence states in dilute alloys has been undertaken. In earlier studies of rare-gas impurities in alkali metals[6] it has been possible to identify specific long-lived excited configurations of the valence shell. These have accurately predictable energies. Work in the same area concerning the interstitial impurities H and O and substitutional Te in alkali metals will be published elsewhere.[12] Paper II of the present series concerns the excitations of halogen impurities. Its particular relevance to the present paper is that the excitations change the ionic charge from $-|e|$ to 0. These are optical charge-transfer excitations which probe directly the stability of the ionic configuration with respect to

nonionic states. It turns out that these total energy differences are in accurate agreement with earlier theoretical predictions.[5]

II. EXPERIMENTAL DETAILS

The specimens used in this work were prepared as thin films by evaporation of the components onto substrates maintained near liquid-He temperature. Concurrent optical work often required that the substrate be a thin single crystal of LiF, in order to obtain optical transmissivity up to a photon energy near 12 eV. Transport measurements merely required that an appropriate electrode pattern be prepared on the substrate prior to the sample evaporation, and for this purpose fused quartz discs proved cheaper than LiF and equally satisfactory. The typical electrode preparation methods and calibration procedures employed in this work are similar to those used in earlier studies of rare-gas impurities, and are described elsewhere.[6]

It was necessary to arrange evaporation conditions in such a way that two samples could be made simultaneously. An evaporation stream of the host metal was allowed to fall equally on both halves of a circular substrate. At the same time, a beam of the second component was channeled up an oblique tube to fall on one half of the substrate only. This arrangement is shown in Fig. 1. The second component was contained within a cooled enclosure, except for a part immediately adjacent to the substrate. This prevented the leakage of solute to the wrong half of the substrate. The dual sample method was most necessary for the optical measurement described in Paper II since a comparison with the pure sample allowed the impurity absorption in the alloy to be isolated. Even for transport measurement, however, it was desirable that a pure metal specimen be prepared to provide appropriate checks on the solvent evaporation.

It deserves mention that the dual source method requires particular care for samples with large resistances. A penumbra formed by either unalloyed metallic component (e.g., in CsSn) can short out a large alloy resistance to produce spurious results. This potential problem can be eliminated by means of appropriate baffles located close to the substrate in order to define the sample shape accurately.

In practice, the best preparation procedure was to adjust both evaporation rates to appropriate values and then to expose the substrate to both beams simultaneously by means of a single shutter. For this purpose the rates were monitored by quartz crystals placed beside the direct path to the substrate. These were precalibrated against
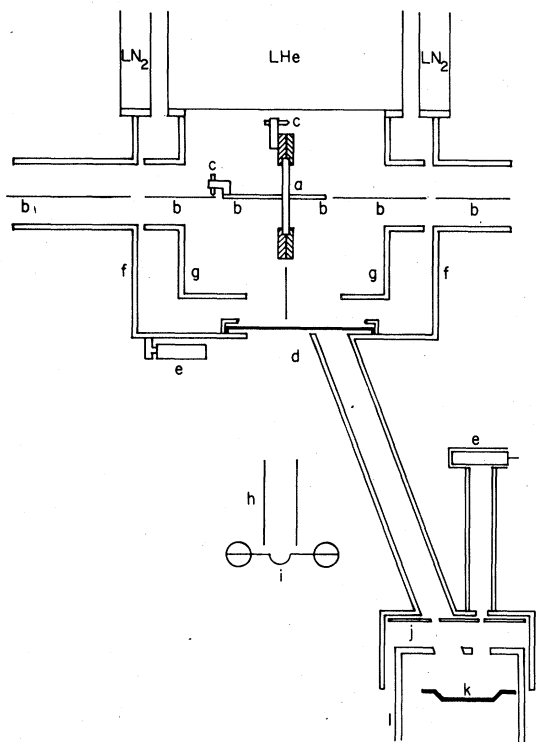
FIG. 1. Cross section of deposition system with radiation shield assemblies connected to liquid-nitrogen (LN$_2$) and liquid-helium (LHe) Dewars: (a) rotatable LiF substrate, (b) light baffles, (c) position indicator, (d) shutter, (e) quartz crystal, (f) liquid-nitrogen radiation shield (g) liquid-helium radiation shield, (h) quartz chimney, (i) alkali-metal evaporation boat, (j) baffle plate, (k) impurity evaporation boat, (l) room-temperature radiation shield surrounding the impurity boat.

crystals temporarily located at the substrate itself, so that the monitor crystals provided an accurate measure of the material falling on the substrate. It was necessary to rely on theoretical calibration constants of the crystals to obtain absolute specimen thicknesses,[13] and these may be in error by as much as 10%. Relative alloy compositions obtained from the ratio of thickness are much more accurate, the uncertainties amounting to 2% at most. Optical measurements of film thickness confirmed the values obtained by crystal calibration within the stated precision.

Alloys prepared in this way proved stable at the typical substrate temperature of 5.5 K. During investigations of the conductivity dependence on temperature it was found that the alloys remained stable up to temperatures ~25 K. Above 25 K, there appear irreversible effects as the lattice evolves towards thermal equilibrium. In the alloys studied here, the solid solubility near He temper-

ature is essentially zero. The equilibration process therefore causes the second component to precipitate either in the form of pure material or intermetallic compound. All the results presented in this paper pertain to samples in which irreversible evolution of the lattice was largely avoided.

The evidence establishing that the alloys remained truly random nevertheless remains fragmentary. A central difficulty is that the specimens cannot be removed either from vacuum or low temperature without spoiling, so that x-ray or other characterization is difficult. In certain cases the results themselves testify to the state of the alloys. Sb-based alloys were not only random but truly amorphous, as exhibited by their observed semiconducting rather than metallic state. In all cases the resistivity varied linearly with alloy composition at dilution, which could not be expected if substantial precipitation occurred in the fabrication process. Perhaps the best evidence for randomness comes from earlier studies of rare gases, in which features of the vacuum uv spectra associated with rare-gas pairs showed the expected composition dependence of amplitude.[14] There nevertheless remains a need for precise methods of sample characterization in this area, particularly with regard to any possible short-range order established at low temperature in codeposited films.

III. RESULTS

Three features of the resistance measurements reported here are of particular interest. They are: (i) the variation of scattering power with impurity species at low impurity concentration (and low temperature), (ii) the variation of resistance with composition in concentrated alloys, and (iii) the effect of temperature change in modifying the resistances observed in (ii). The very wide choice of available solute and solvent species ruled out any possibility of exhaustive study. Much of the present work was therefore focused on Cs-based alloys, for which ionic effects are expected to be most widespread because of the low ionization potential of Cs. Some data were then taken for Na- and Rb-based alloys to provide a comparison with the Cs data.

We interpret the observed resistances as characteristics of homogeneous films thick enough to eliminate surface perturbations from the observed values. Most measurements were in fact made on films 1000–2000 Å thick. Some halogen systems were studied with 500-Å films but, even then, the mean free paths near the metal-insulator transition are much shorter, and the current is, in any case, channeled along percolation paths so that

surface effects are eliminated. Furthermore, in-
dependent studies have shown that film inhomo-
geneities cease to have a major influence on the
resistance of films more than 250 Å thick.[15] Our
films were very much thicker. The resistivities
have therefore been derived directly from the ob-
served resistances using film thicknesses calcu-
lated from the atomic surface density together with
Vegard's law for the molar volume. Minor uncer-
tainties of this type in film thickness have little im-
portance when the resistance varies over many or-
der of magnitude, as in the present work.

Figures 2, 3, and 4 provide an overview of the
resistivity changes caused by the alloying Cs with
Ag, Cd, In, Sn, Sb, Te, I, and Xe, i.e., one com-
plete row of the Periodic Table. The Xe data are
taken from earlier studies reported by this re-
search group.[7] A number of interesting features
of the data deserve comment. First, the resist-
ance varies linearly with impurity concentration
in the dilute limit as expected from the fact that
impurities then scatter independently. Figure 5
shows the data on a linear, expanded scale that
makes the proportionality more evident. The
slopes of the lines give the residual resistivities,
which measure the scattering power per impurity.
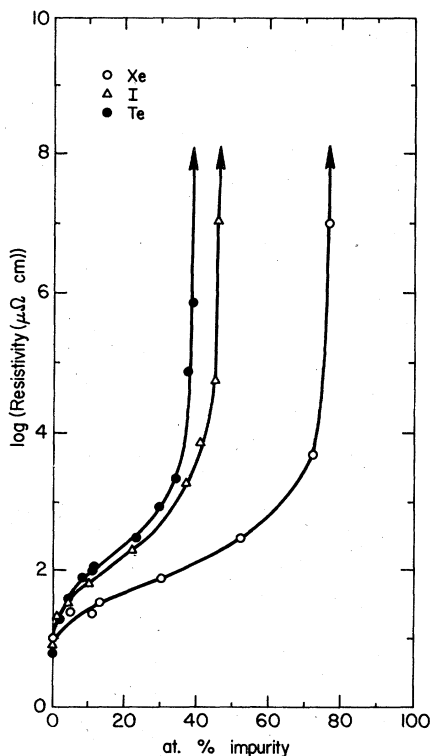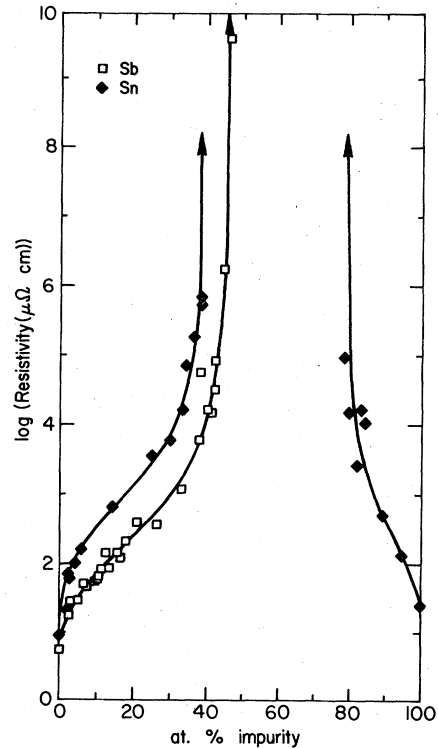The numerical values are collected in Table I and

FIG. 3. Resistivity of CsSb and CsSn alloys as a func-
tion of Sb and Sn concentrations. Note the region between
~39 and ~82 at.% Sn where the CsSn alloys remain in-
sulators.

displayed as a function of impurity valence in Fig.
6. We shall return in Sec. IV to discuss the strik-
ing changes of resistance with impurity species
apparent in Fig. 6.

The second feature revealed by the data in Figs.

FIG. 2. Resistivity as a function of Xe, I, and Te
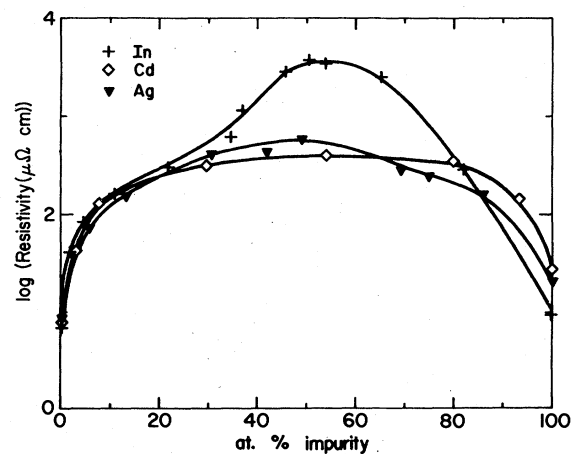impurity concentrations in CsXe, CsI, and CsTe alloys.

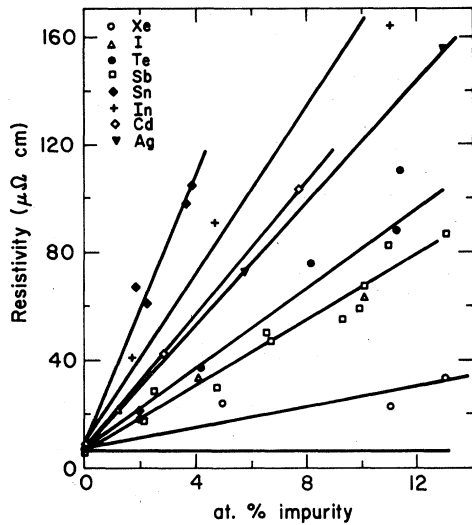FIG. 4. Resistivities of Cs alloys as a function of Ag,
Cd, and In compositions.

FIG. 5. Linear variation of resistivity with impurity concentration in Cs-based alloys for Ag, Cd, In, Sn, Sb, Te, I, and Xe impurities.
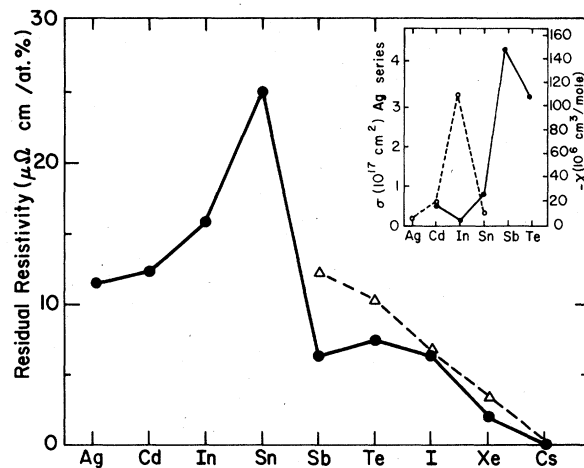

FIG. 6. Residual resistivity introduced by 1 at.% of Ag-row impurities in Cs host at 5.5 K. The molar susceptibility[3] and the spin-flip scattering cross section[2] σ of Ag-row impurities in the Na host are shown inset in the figure. The broken line between Xe and Sn is calculated for a hard-sphere model (see text).

2, 3, and 4 is that the impurities Sn, Sb, Te, I, and Xe each cause the material to become an insulator when present beyond a specific critical composition c_c which differs from one solute species to the next. The critical compositions are not related in a simple way to the solute valence or to its residual resistivity. They will be discussed later in connection with impurity charge-transfer states. For the moment we merely note that the resistance variation with c near c_c has a similar appearance in all cases for which a transition occurs. It is worth remarking that the sample resistances exceed the 10^3-MΩ limit of our equipment at compositions slightly exceeding c_c. Thus, the critical composition itself is, in each

case, fixed to better than ~2% by the data.

In a number of cases the resistance variation near the transition depends mainly on the impurity valence. This has previously been demonstrated for Xe in Cs and Kr in Rb.[7] The analogous results for I in Cs and Br in Rb are presented in Fig. 7. This close identity of behavior does not extend to a complete dependence on chemical type alone, as revealed by Fig. 8. It can be seen there that the residual resistances of F and Br in Rb differ appreciably, as also do Br and I in Cs. In each case the larger ion gives the greater resistance. These residual resistance data are collected in Table I, also.

TABLE I. Residual resistivities of impurities in alkali metals at ~5.5 K.

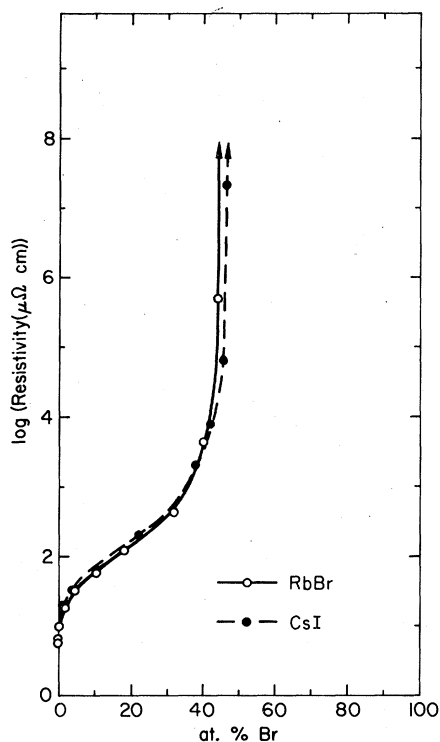| Host	Impurity	Residual resistivity ($\mu\Omega$ cm)/at.%	Host resistivity ($\mu\Omega$ cm)
	Xe	2.0 ± 0.5	
	I	6.3 ± 1.0	
	Te	7.4 ± 1.0	
	Sb	6.3 ± 1.0	7
Cs	Sn	25.0 ± 2.0	
	In	15.6 ± 2.0	
	Cd	12.2 ± 1.0	
	Ag	11.4 ± 1.0	
	Br	4.0 ± 1.0	
Rb	Br	6.0 ± 1.0	6.5
	F	3.6 ± 1.0	
Na	Sn	25.7 ± 2.0	4

FIG. 7. Resistivity of Rb-Br and Cs-I alloys as functions of Br and I concentrations.

The case of CsSn is of particular interest because it exhibits two metal-insulator transitions. It is, of course, expected that Cs-rich and Sn-rich materials are both conductors. The novel point is that the CsSn mixtures make a perfectly insulating phase over the composition range between 38 at. % and 78 at.% Sn. The occurrence of the phase depends delicately on properties of the two component species. This is evident from the
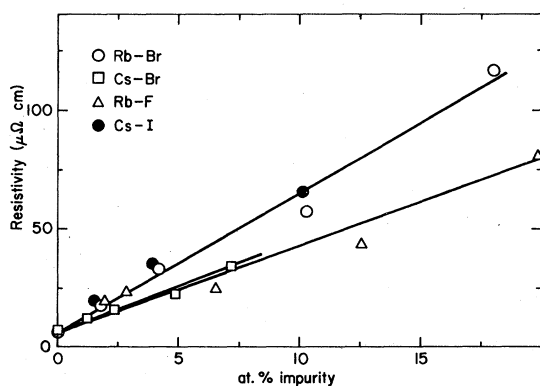

FIG. 8. Resistivities of Rb-Br, Rb-F, Cs-Br, and Cs-I alloys as a function of halogen compositions.

comparison of NaSn data with CsSn data in Fig. 9. A still weaker transition occurs for CsAu, as shown in Fig. 10. In the latter case it was not possible to make alloys with a truly infinite resistance owing, no doubt, to the very narrow composition range over which large resistances occur.

It is particularly noticeable in the cases of CsAu and NaSn that rapid resistance increases occur when the observed value reaches about 3×10^3 $\mu\Omega$ cm. An examination of the remaining data shows that this is true for Sb, Te, I, and Xe, also. The case of CsIn is of special interest in this connection. Figure 4 shows that the peak resistance occurs close to this same critical value, but without any signs of a sharp transition to the insulating phase and back. We conclude that CsIn is very close to a metal insulator transition at 50 at.% composition, but either does not reach the insulating phase, or our preparation methods proved inadequate to fabricate the ideal 50 at.% insulators. CsSb certainly becomes insulating near 46 at.% Sb, but fails to become conducting again at high Sb concentrations. An investigation of the temperature dependence of conduction in pure Sb films showed that they were semiconducting (Fig. 11), in agreement with other reports that evaporated
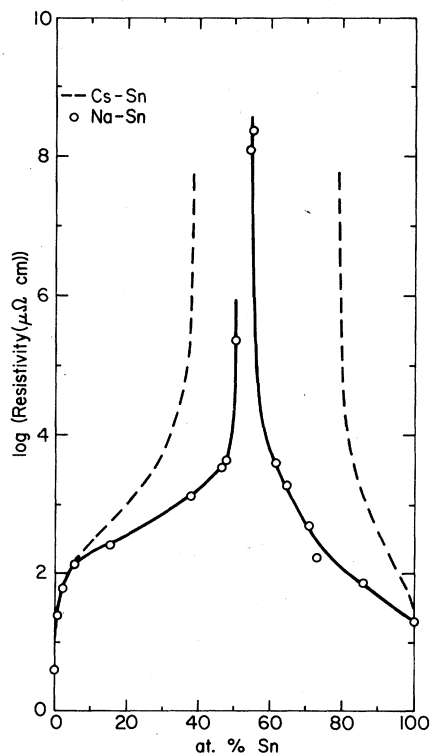

FIG. 9. Change in resistivity of NaSn alloys as a function of Sn concentration. The broken line represents CsSn data (see Fig. 3) for comparison.
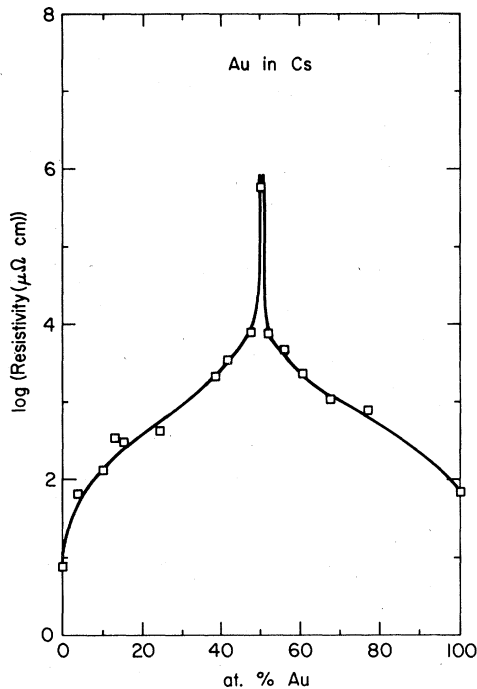
CHARGE TRANSFER AND PERCOLATION IN ALKALI ALLOYS

FIG. 10. Resistivity of CsAu alloys as a function of Au concentration.

Sb is an amorphous semiconductor.[16] Evidently the return to the metal phase at high Sb concentration in CsSb is prevented by short-range disorder of this type.
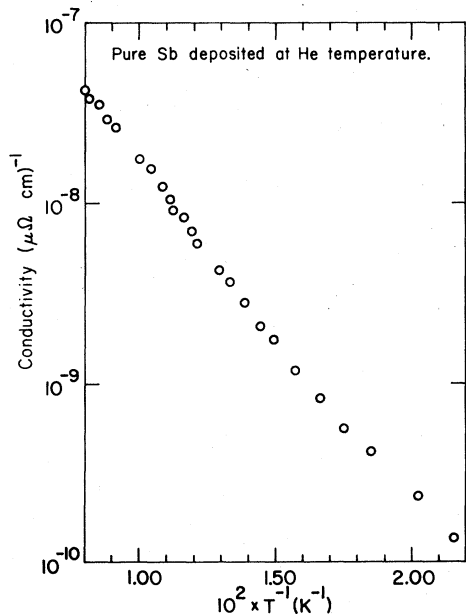
In measurements of temperature dependence we have confirmed that the resistances of these materials appear temperature sensitive whenever the resistance exceeds 10^4 $\mu\Omega$ cm for the thickness of film that proved convenient in this work. Presumably the sharp transition regions to the insulating phase with $\rho \gtrsim 10^4$ Ω in Figs. 2–4 contain resistances that are in some degree temperature dependent. These effects have been documented in our laboratories for rare-gas and halogen impurities by Durbin, and will be reported here for several of the more complex materials.

Figures 12, 13, and 14 show for some CsSn, NaSn, and CsAu alloys the observed temperature dependence of resistance. In the two latter cases the warming cycle was continued too far and small irreversible changes of resistance took place. In some of these figures it is apparent that conductivities $\sim 10^{-4}$ $(\mu\Omega$ cm$)^{-1}$ are accompanied by only small factional changes of resistance with temperature. However, the temperature effect becomes very significant when the conductivity falls below the 10^{-5} to 10^{-6} $(\mu\Omega$ cm$)^{-1}$ range. It is particularly noteworthy that for the present choice of film thickness this conductivity range corresponds to actual specific surface resistivities near 3×10^4 $\Omega/\square$.

A final point of some interest concerns superconductivity in the In- and Sn-rich Na- and Cs-based materials. Figure 15 gives data for 71 at.% Sn in Na. The temperature-independent metallic

FIG. 11. Temperature variation between 35 and 85 K for conductivity of a pure antimony metal film (~314 Å thick) deposited onto a cold substrate at He temperature.

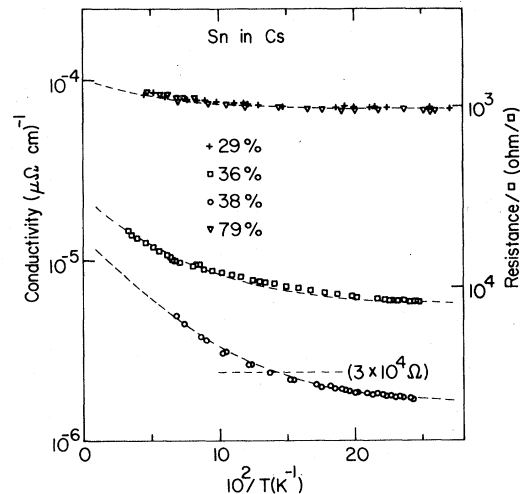FIG. 12. Temperature dependence of conductivity in some CsSn mixtures containing 19, 36, 38, and 79 at.% Sn. The horizontal broken line marks the theoretical limit for minimum metallic conductivity[15, 22, 23] in two dimensions. The broken lines passing through the experimental curves are theoretical fits to Eq. (6).
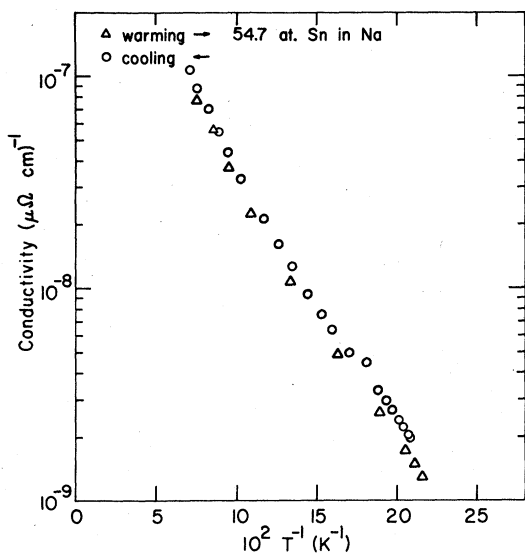
FIG. 13. Temperature variation of conductivity in NaSn alloys having ~55 at.% Sn. Data points corresponding to "cooling" and "warming" cycles are indicated separately.
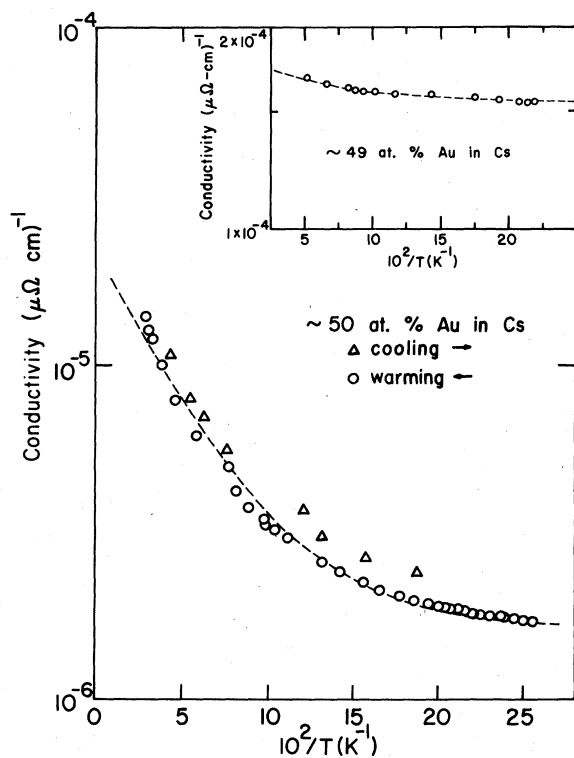

FIG. 15. Resistivity variation of NaSn as a function of temperature at 71 at.% Sn concentration.

FIG. 14. Temperature variation of conductivity in a CsAu alloy at stoichiometric composition (~50%). Cooling and warming cycles are indicated. The dashed line corresponds to the theoretical fit to Eq. (6). The inset in the figure shows $\sigma(T)$ for a 49 at.% CsAu alloy.
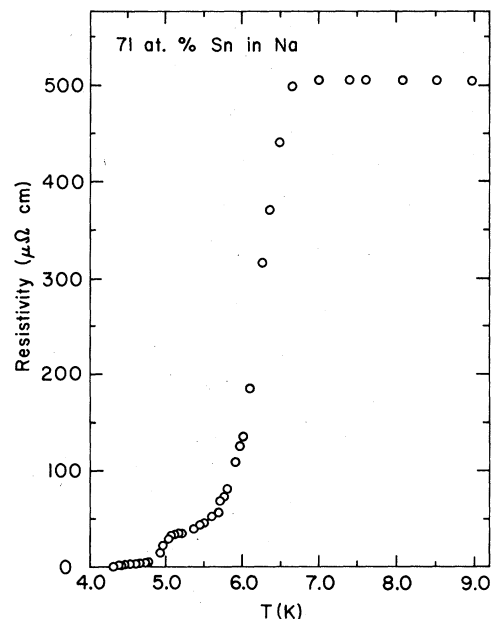
conductivity above 7 K is broken by a broad transition centered at 6 K, and the resistivity tends to zero near 5 K. This behavior is typical of broadened superconductivity transitions observed in inhomogeneous samples, and it is to be expected that the material near a percolative transition is indeed inhomogeneous on a microscopic scale. It is also noteworthy that the transition temperature in the alloy exceeds that of pure Sn.

The superconductivity competes with hopping process in materials close to the metal-insulator transition. Figure 16 shows by way of example how the conductivity passes through a minimum as a function of temperature in Na 47.6 at.% Sn. The conductivity increases below 5 K in a broadened superconducting transition and shows, in addition, the increase at higher temperatures expected from hopping conduction in materials with resistivities $\gtrsim 10^4$ $\mu\Omega$ cm.

IV. DISCUSSION

A. Charge-transfer effects

The phenomenon of major significance in the present work is charge transfer. This effect influences the observed resistances in three ways. First, the transfer of electrons from band states to core orbitals can deplete the conduction-electron density below the level required to support charge percolation. Second, the critical impurity compositions at which the simpler metal-insulator
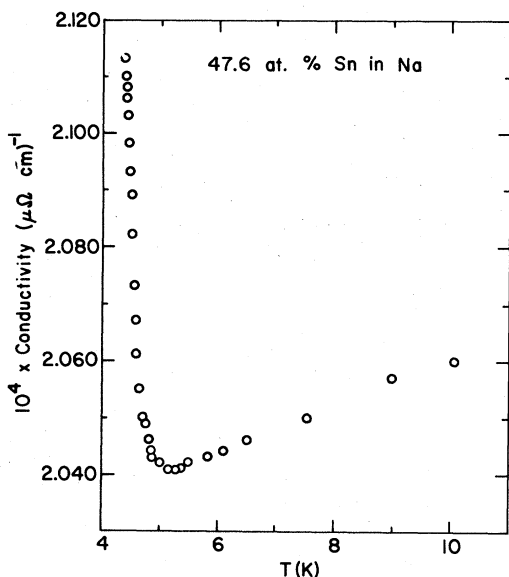
FIG. 16. Conductivity variation with temperature for 48 at.% Sn in Na.

transitions occur are close to those required for exact charge transfer from alkali to solute atoms. As a result, the positions of these transitions are determined by the solute valence. Third, the observed residual resistivities, which are fixed by the impurity scattering power and hence its structure, depend in a striking way on the occurrence of charge transfer. The qualitative feature of these several properties are considered briefly in what follows.

Figure 6 shows the degree to which charge transfer influences transport properties in dilute alkali alloys. Inset are spin-flip scattering cross sections[2] and impurity susceptibilities[3] for Ag-row impurities in Na (liquid). The main figure gives the present results for the resistance of these same impurities in solid Cs.

We neglect host-induced differences to focus attention on the qualitative way in which the spin-flip scattering and resistance suddenly decrease at the point at which the giant diamagnetism appears. Both spin-flip and resistance scattering measure the coupling of band states to the core. Both decrease abruptly between In and Sb because charge transfer occurs and the conduction electrons then scatter off the repulsive long-range Coulomb field rather than the ion core. At the same time, the large diamagnetism arises from the spread of the weakly bound core orbitals and the negative density of band states caused by the ionic repulsion, as explained by Flynn and Lipari.[4] The composite data identify unambiguously a qual-

itative change of impurity structure in passing from In to Te.

The same conclusions can be reached from the data for the metal-insulators transitions. With Xe in Cs the transition occurs at 78 at.% Xe. This is very close to the value predicted by simple percolation models (see Sec. IV C below). Equal numbers of Cs and I atoms are required for exact charge transfer, and a small excess of Cs atoms is needed for percolation. This agrees with the observed I concentration of 45% at the metal-insulator transition. Similarly, the transition with divalent Te is expected on the Cs-rich side of the 2 : 1 atom ratio. Its occurrence at 39% Te rather than <33% Te may indicate that the Te 5p orbitals overlap enough to assist charge transport so that charge transfer is incomplete. Nevertheless, this case fits well with the broad scheme of charge-transfer effects. The resistance of the Cs-In system shows no metal-insulator transition; the charge-transfer insulating phase is, at most, insipient near 50 at.% In. With I and Te singly and doubly charged ions, respectively, and In uncharged, we thus reach the same conclusions from the transition data as those arrived at above from the residual resistance: a transition from the normal to the charge-transfer impurity configuration occurs between In and Te.

A superficial interpretation of the transition results would suggest that Sn and Sb take the configurations Sn^{2-} and Sb^-, since their critical compositions are close to those of Te^{2-} and I^-, respectively. Evidently these are intermediate cases between zero and complete charge transfer. Their structures are, however, likely to be more complicated than is immediately apparent, since incomplete charge transfer involves a breakdown of the 5p shell degeneracy implied in one-electron theories.

In concluding this qualitative discussion of the data it is of interest to inquire whether any evidence accurately identifies the point at which, with increasing solute valence, the full impurity orbitals emerge from the band bottom. The answer is that the concept of localized states pertains only to one-electron descriptions and its significance can be blurred by the nonaverage Coulombic interactions in real materials.[17] To identify state energies one can only discuss excitation spectra which are broadened by recombination processes in real cases. The specific results obtained in the present work appear to show that this natural limitation is complicated further by static Coulomb correlations manifested by incomplete charge transfer in the transitional region. Nevertheless, the domain in which these charge-transfer effects occur is in accurate agreement with the theoretical predictions by Flynn and Lipari.[4]

B. Residual resistance

One cannot expect to calculate accurate residual resistances for impurities, even in alkali metal hosts. Theories of the residual resistance have met with semiquantitative success at best. In the free-electron model of an isotropic metal containing a spherically symmetrical impurity potential the residual resistivity may be written

$$\rho = A \sum_l (l+1) \sin^2(\eta_{l+1} - \eta_l) , \qquad (1)$$

with η_l and l wave phase shift for an electron at k_F scattering off an impurity, and

$$A = 4\pi\hbar/e^2 k_F . \qquad (2)$$

This formula reproduces with 20% accuracy the observed resistance in a number of alloys, given appropriate phase shifts.[18] The latter require a self-consistent (nonlinear) treatment of the impurity-host complex, which involves a delicate balance of energies in the present case of charge-transfer centers. In addition, Fukai has shown that significant corrections to Eq. (1) are necessary (in the cases of Pb and Al hosts) to account for the effect of Bragg diffraction on impurity scattering.[19] Neither accurate phase shifts nor a detailed dynamical model of scattering in Cs is available at present, so accurate predictions are out of the question.

What we shall do instead is to show that the resistances of some particular impurities are consistent with their chemical description explained above. The connection between the phase shifts and the chemistry is the Friedel sum rule

$$\mathcal{Z} = \sum \mathcal{Z}_l = \sum 2(2l+1)\eta_l/\pi , \qquad (3)$$

linking the screening charge $\mathcal{Z}_l$ in l waves to the l-wave phase shift.[18] We choose Ag, Xe, and Sn as impurities typical of the left, right, and center of the row in the Periodic Table. The observed resistances span a factor ~10 in magnitude, and include the unexpectedly large (and hitherto unexplained) resistance introduced by monovalent noble metals in monovalent alkali metals. To explain these resistances we use only s and p waves, and a value of the constant A close to that predicted by Eq. (2). The three impurities are considered successively in what follows.

Xe: This small atom would have $\mathcal{Z} = -1$ in the absence of lattice relaxation. We guess that $\mathcal{Z} \simeq -\frac{3}{4}$ (25% relaxation) and that the screening is mainly accomplished by s waves (as is typical for compact repulsive potentials). With $\eta_0 = -34°$, $\eta_1 = -11°$, and $\eta_l = 0$ $(l>1)$, one obtains $\mathcal{Z} = -0.74$ and

$$\sum_l (l+1) \sin^2(\eta_l - \eta_l) = 0.23 . \qquad (4a)$$

Sn: The resistance is so large that the p waves must be nearly resonant. Also, $\mathcal{Z} = +3$ in order that the excess charges of Sn in Cs be screened. With $\eta_0 = 15°$, $\eta_1 = 85°$, and $\eta_l = 0$ $(l>1)$ one obtains $\mathcal{Z} = +3.0$ and

$$\sum_l (l+1) \sin^2(\eta_{l+1} - \eta_l) = 2.87 . \qquad (4b)$$

Ag: The large resistance of noble metals in alkalies has previously lacked an explanation. A clue is provided by the charge transfer revealed for CsAu in Fig. 10. Evidently the affinities ~2 eV of noble metals make them tend to occupy the $(s^2)^-$ ionic configuration when mixed with the alkali. This s electron attraction must be compensated by a p-wave repulsion (the s-p splitting of noble metals exceeds the Cs bandwidth). With $\eta_0 = +75°$, $\eta_1 = -25°$, and $\eta_l = 0$ $(l>1)$, one obtains $\mathcal{Z} = 0$ and

$$\sum_l (l+1) \sin^2(\eta_{l+1} - \eta_l) = 1.33 . \qquad (4c)$$

The summations in Eqs. (4) are collected in Table II. Their ratios to the experimental resistances define an "empirical" value of the constant in Eq. (2) as $A = 8.6$ $\mu\Omega$ cm/at.%, which gives the satisfactory prediction shown in Table II. The theoretical value of A obtained from Eq. (2) directly is 8.1 $\mu\Omega$ cm/at.%. This is in as good agreement with the deduced value as could be desired. Phase shifts can evidently be chosen to be simultaneously consistent with the impurity chemistry, the observed resistances, and the parameters of the host electron gas. Their probable energy dependences are sketched in Fig. 17 for the three impurities discussed here.

Questions of charge transfer enter the above calculations only for the s-wave case of Ag. It is therefore of interest to examine also the case of p-wave charge transfer relevant to I^-, Te^{2-}, and Sb^{3-} in Cs. Even the simplest model is rather effective. We represent the impurity by an infinite repulsive barrier of radius a chosen to satisfy the Friedel sum rule for the appropriate negative ion. The phase shifts are then

TABLE II. Collection of phase shifts η_0 and η_1, Friedel sums Z, and the resistivity summations Σ_l in Eq. (4). The resistivities ρ_{th} obtained from these summations with $A = 8.6$ $\mu\Omega$ cm/at.% in Eq. (3) are compared with the observed values ρ_{exp} ($\mu\Omega$ cm/at.%).

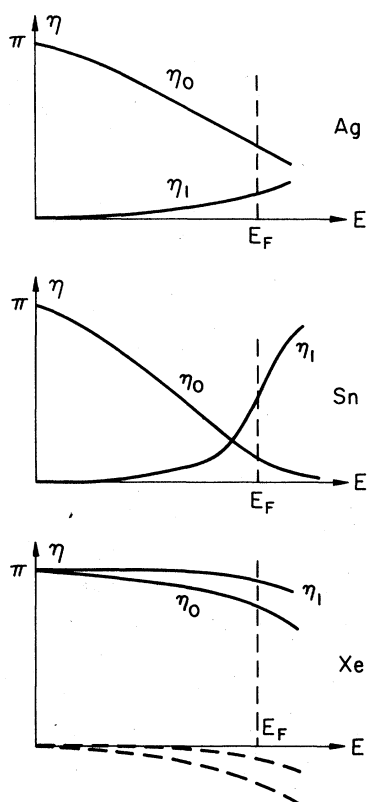|	η_0	η_1	Z	Σ_l	ρ_{th}	ρ_{exp}
Ag	75°	−25°	0	1.33	11.4	11.4
Sn	15°	85°	3	2.87	25	24.7
Xe	−34°	−11°	−0.74	0.23	2.0	1.9

FIG. 17. Sketches showing possible energy dependencies of phase shifts for Ag, Sn, and Xe, consistent with the values at E_F discussed in the text. For Xe, values reduced by π are indicated by broken lines, to show the analogy with a weak repulsive scatterer.
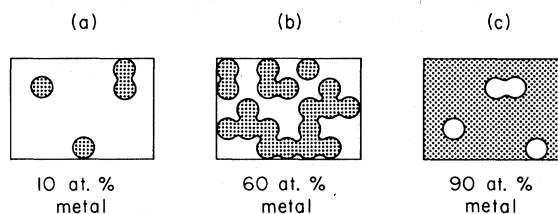

FIG. 18. Sketch showing the valence-electron distribution in alkali metals containing charge-transfer impurities at various concentrations. The diagram shows that a strong similarity exists between the alloy and a macroscopic percolative mixture (drawn for the example of rare-gas impurities).

$$\eta_l = j_l(k_F a)/n_l(k_F a) \,, \tag{5}$$

with j_l and n_l spherical Bessel functions. As shown in Fig. 6, the resulting estimates provide a satisfactory order-of-magnitude fit to the observed resistivities of Xe, I, and Te impurities in Cs.

The preceding discussion may be summarized by the comment that the observed residual resistivities are quantitatively consistent with the charge-transfer characteristics deduced from chemical arguments. A prediction from first principles must await the calculation of accurate phase shifts by self-consistent methods.

C. Metal-insulator transitions

In circumstances of strongly favored charge transfer the valence orbitals of the electron acceptor lie below the band bottom of the alkali host metal. They form completely localized full shells. The conduction must then be associated with the remaining occupied alkali orbitals. This is certainly the case for Xe° and I^- in Cs, and it probably

remains substantially true for Te^{2-} also. Conduction electrons are repelled from these foreign ions and thereby confined to alkali sites. The effect of this confinement is sketched in Fig. 18. It is the topology of conducting paths between neighboring alkali atoms that determines charge transport. The transition to the insulating phase must resemble that in macroscopic models of percolation through mixtures of conducting and nonconducting balls. Arguments of this type were first presented by Phelps et $al.$ for the CsXe and RbKr systems.[7]

The generally similar forms taken by the several metal-insulator transitions close to their critical compositions suggest that much the same phenomena occur at each. This similarity conforms rather well in many cases to the theoretical scaling law prediction[20] that the resistance behaves as a power law:

$$\rho \propto (c - c_c)^{-s} \quad (c \to c_c)$$

close to c_c. Figure 19 shows how appropriate choices of c_c within the experimental latitude of $1\% - 2\%$ do give plots of $\log \rho$ vs $\log(c - c_c)$ that yield presentably straight lines. For the systems with strongly favored charge transfer the slopes of the lines are a little greater than 2.0. For less well bound configurations the average rises to a about 3. The average of $s = 2.1 \pm 0.1$ among rare-gas, halogen, and Te impurities agrees better with the prediction $s = 2.0$ of Adler[20] than the well-documented value $s = 1.6 \pm 0.1$ proposed by Kirkpatrick.[21]

When account is taken of the temperature dependence of resistance observed in alloys with $\rho \gtrsim 10^4$ $\mu\Omega$ cm, the significance of the observed values of s becomes questionable. The observed temperature dependences are, however, very interesting, particularly in relationship to the concept of a minimum metallic conductivity for films.[22] In this connection we mention that the lines shown drawn
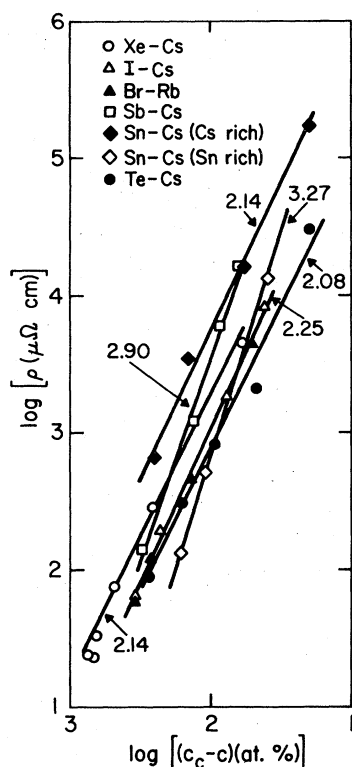
FIG. 19. Logarithm of the resistance plotted as a function of $\log(c_c - c)$, with c the impurity composition and c_c the composition at which the material becomes an insulator. The numbers associated with the lines give the slopes s.

through the data points in Figs. 12 and 14 represent fits to an assumed form

$$\sigma = \sigma_0 + \sigma_a \exp(-E/kT) \qquad (6)$$

for the conductivity. This equation represents metallic and thermally activated portions acting in parallel. The fits to the assumed form are quite adequate. The values of σ_a, σ_0, and E obtained

from these fitting procedures are collected in Table III. Two interesting observations may be made. First, all the data are well described by an activation energy for hopping of about 2 meV. Second, the data strongly support the idea of a maximum metallic resistance close to the theoretical value of 3×10^4 Ω. In the three cases for which $\sigma_0 \lesssim 3 \times 10^{-5}$ $(\mu\Omega$ cm$)^{-1}$, the data in Figs. 12, 13, and 14 show that the conductance is mostly due to thermal activation. Data taken at lower temperatures would clearly be of interest in fixing the precise limit of the metallic state. In this connection, we note that the percolative materials studied here present special theoretical problems since their filiamentary character near c_c makes them resemble single strands as much as conducting sheets. Existing theories give rather different results for the resistance in the two cases.[22,23] The assumed form (6) for the conductivity implies that activated paths cross link the percolation chains. In view of the small deduced activation energies (near 2 meV) one might infer that these links are, in fact, metal strands that have transformed to the hopping regime of conduction. Certainly, the values of E in this range are much too small to describe hopping through insulating regions of Xe or I in the percolation limit near c_c.

D. Charge-transfer insulators

Perhaps the most interesting result of this work is the observation that disordered regions of the charge-transfer insulator phase exist in several of the phase diagrams investigated here. These are disordered materials in which charge transfer from one component to the second reduces the available number of carriers below the level needed for percolation. We conclude this paper with brief comments on the nature of these materials.

Clearly the alkali-metal−halogen alloys appear to conform ideally to the simplified concept of a

TABLE III. Activation energy E and conductivity components σ_0 and σ_a, used to fit the observed conductivity σ using Eq. (6).

Alloy	E (eV)	σ_0 $(\mu\Omega^{-1}\,cm^{-1})$	σ_a $(\mu\Omega^{-1}\,cm^{-1})$
29 at.% Sn in Cs	1.6 10^{-3}	7.00 10^{-5}	3.00 10^{-5}
36 at.% Sn in Cs	1.6 10^{-3}	5.75 10^{-6}	1.63 10^{-5}
38 at.% Sn in Cs	1.6 10^{-3}	1.60 10^{-6}	1.15 10^{-5}
79 at.% Sn in Cs	1.6 10^{-3}	7.00 10^{-5}	3.00 10^{-5}
82 at.% Sn in Cs	~1.6 10^{-3}	~3.61 10^{-5}	~3.50 10^{-5}
55 at.% Sn in Na	~2.4 10^{-3}	0	⋯
49 at.% Au in Cs	~1.2 10^{-3}	1.56 10^{-4}	2.60 10^{-5}
50 at.% Au in Cs	2.0 10^{-3}	1.65 10^{-6}	2.00 10^{-5}
Amorphous Sb	~36.7 10^{-3}	0	~10^{-6}

disordered ionic material. In the range between 45% and 50% halogen in CsI, for example, these solids undoubtedly comprise I^- and Cs^+ atoms with insufficient Cs^0 to support conduction. Additions of I beyond 50% will probably increase the I_2 molecule density (H and V centers). In the materials prepared here, the presence of I_2 in alloys with $c < 50$ at.% I is made unlikely by the preparation method, using the salt evaporation.

In the case of CsTe alloys, it is quite possible that local fluctuations in Cs and Te concentrations produce a fraction of sites for which ideal charge transfer becomes blocked. Effects of this type could explain why the transition to the insulating phase occurs near 39 at.% Te instead of $\lesssim 33$ at.%. Any suppression of charge transfer produces excess Cs^0 and Te^- to promote conduction. Regions containing excess Te^0 presumably bond in much the same way as solid Te. With a greatly increased Te concentration the material must tend to consist of $Cs^+ Te^-$ complexes in solid Te. Some evidence for Te pairing effects has been observed in the optical spectra of Te in Cs.[12]

Sn and Sb alloys with Cs are more complicated. Were crystalline Sb, rather than amorphous Sb, produced by evaporation, both systems would undoubtedly exhibit a bounded range of the charge-transfer insulating phase. In practice CsSn alone reveals this interesting property because evaporated Sb is an insulator at 5 K. The domain of the phase is greatly reduced when Cs is replaced by Na to make NaSn, presumably because Na is small and less reactive than Cs. In CsAu this domain is still smaller. Nevertheless, transport measurements in the liquid have revealed that the charge is carried by Au^- and Cs^+ ions in alloys with compositions near 50 at.%,[9] so this material also is a charge-transfer insulator. It seems likely that the Sn affinity (1.25 eV) is sufficient to make it generally ionic, also, in both Cs and Na. In view of the large change in the extent of the phase existence with a change of cation from Cs to Na, one must deduce that the charge transfer is rather delicately balanced, and probably involves cooperative rather than pairwise charge exchange. Certainly, a large excess of either Cs or Sn is required to produce conductivity in CsSn, whereas only a small excess of either component is needed in NaSn.

We note in conclusion that x-ray studies show energy gaps ~2 eV in ordered crystals of CsAu.[24] It is apparent from the present experiments and those on liquids, however, that translational symmetry is not the major influence on the excitation spectrum of this material. The main effect is charge transfer; both the ionicity and the excitation gap are maintained even in the disordered state. This confirms the results of Kitter and Falicov.[25] These authors show theoretically that a band gap opens up at E_F in equiatomic CsAu disordered mixtures when the probability of Au-Au near neighbor pairs falls below about 0.36. The probability in a perfectly random mixture is 0.25 and that in the ordered compounds zero. From the small apparent band gap in Figs. 10 and 14 one might infer that the actual material investigated here lies in the upper part of the insulating range, rather close to ideal randomness.

---

[1] See, for example, M. A. Bredig, in *Molten Salt Chemistry*, edited by M. Blander (Wiley-Interscience, New York, 1964).

[2] M. A. Ball, J. R. Asik, and C. P. Slichter, Phys. Rev. 181, 662 (1969).

[3] C. P. Flynn and J. A. Rigert, Phys. Rev. B 7, 3656 (1973).

[4] C. P. Flynn and N. O. Lipari, Phys. Rev. Lett. 27, 1365 (1971).

[5] C. P. Flynn, Phys. Rev. B 9, 1984 (1974).

[6] D. J. Phelps, R. A. Tilton, and C. P. Flynn, Phys. Rev. B 14, 5254 (1976). References to other work on rare gas-metal alloys will be found in this paper.

[7] D. J. Phelps and C. P. Flynn, Phys. Rev. B 14, 5279 (1976).

[8] See, e.g., Ref. 2 for some collected results.

[9] W. Freyland and G. Steinleitner, Inst. Phys. Conf. Ser. 30, 488 (1977); Ber. Bunsenges Physik. Chem. 80, 810 (1976).

[10] H. Hoshino, R. W. Schmutzler, and F. Hensel, Phys. Lett. A 51, 7 (1975); Ber Bunsenges Physik. Chem. 80, 107 (1976).

[11] K. D. Kruger, R. Fisher, and R. W. Schmutzler, Inst. Phys. Conf. Ser. 30, 480 (1977); Ber. Bunsenges. Physik. Chem. 80, 816 (1976).

[12] R. P. Layton, Ph.D. thesis (University of Illinois, 1976) (unpublished).

[13] W. H. Lawson, J. Sci. Instrum. 44, 917 (1976).

[14] R. A. Tilton, D. J. Phelps, and C. P. Flynn, Phys. Rev. B 14, 5265 (1976).

[15] R. C. Dynes, J. P. Garno, and J. M. Rowell, Phys. Rev. Lett. 40, 497 (1978).

[16] J. J. Hauser, Phys. Rev. B 11, 738 (1975); 9, 2923 (1974).

[17] N. F. Mott, Proc. Met. Phys. 3, 76 (1952); J. Phys. Radium (Paris) 23, 594 (1962); W. Kohn and

C. Majumder, Phys. Rev. A **138**, 1677 (1965).

[18]For a discussion and references see, for example, C. P. Flynn, *Point Defects and Diffusion* (Clarendon, Oxford, 1972), p. 742.

[19]Y. Fukai, Phys. Rev. **181**, 647 (1969).

[20]D. Adler, L. P. Flora, and S. D. Senturia, Solid State Commun. **12**, (1973).

[21]S. Kirkpatrick, Phys. Rev. Lett. **27**, 1722 (1971).

[22]D. C. Licciardello and D. J. Thouless, Phys. Rev. Lett. **35**, 1475 (1975); T. Lukes and R. S. Tripathi, Philos. Mag. **36**, 1533 (1977); see also Ref. 15.

[23]D. J. Thouless, Phys. Rev. Lett. **39**, 1167 (1977).

[24]W. E. Spicer, A. H. Sommer, and J. G. White, Phys. Rev. **115**, 57 (1959).

[25]R. C. Kittler and L. M. Falicov, J. Phys. C **9**, 4259 (1976).